NANO LETTERS

2006
Vol. 6, No. 9
2109−2114

Optically Driven Resonance of Nanoscale Flexural Oscillators in Liquid

Scott S. Verbridge,[†] Leon M. Bellan,[‡] Jeevak M. Parpia,[†] and H. G. Craighead*[,‡]

Department of Physics and the Cornell Center for Materials Research, Cornell University, Ithaca, New York 14853, and School of Applied and Engineering Physics and the Cornell Center for Materials Research, Cornell University, Ithaca, New York 14853

Received June 19, 2006; Revised Manuscript Received August 7, 2006

ABSTRACT

We demonstrate the operation of radio frequency nanoscale flexural resonators in air and liquid. Doubly clamped string, as well as singly clamped cantilever resonators, with nanoscale cross-sectional dimensions and resonant frequencies as high as 145 MHz are driven in air as well as liquid with an amplitude modulated laser. We show that this laser drive technique can impart sufficient energy to a nanoscale resonator to overcome the strong viscous damping present in these media, resulting in a mechanical resonance that can be measured by optical interference techniques. Resonance in air, isopropyl alcohol, acetone, water, and phosphate-buffered saline is demonstrated for devices having cross-sectional dimensions close to 100 nm. For operation in air, quality factors as high as 400 at 145 MHz are demonstrated. In liquid, quality factors ranging from 3 to 10 and frequencies ranging from 20 to 100 MHz are observed. These devices, and an all-optical actuation and detection system, may provide insight into the physics of the interaction of nanoscale mechanical structures with their environments, greatly extending the viscosity range over which such small flexural resonant devices can be operated.

Because of their extreme sensitivity to external forces, small mechanical resonators have been used in a number of sensing applications. Biological masses approaching the single-molecule level have been detected.[1] Tapping-mode atomic force microscopy (AFM) has allowed for high-resolution imaging of soft materials.[2] The properties of the environments in which these resonant devices are operated have also been measured, including viscosity and gas composition, pressure, and temperature.[3] In all of these applications, it is useful to be able to operate the sensing resonator in as wide a range of environmental conditions as possible, while utilizing the smallest possible resonator for maximum sensitivity to forces. When operating resonant devices of shrinking dimensions in the sorts of viscous environments most relevant to biological systems, such as water or buffer solutions, losses resulting from viscous drag become sizable in comparison with the total energy stored in the resonant motion. This problem of viscous damping has prevented truly nanoscale flexural resonators, with cross-sectional dimensions on the order of 100 nm, from being operated in liquid environments.

We demonstrate the operation of flexural nanoscale resonators in air, as well as liquids including alcohol, water, and buffer. A thin metal layer is used in conjunction with an optical drive technique to increase the driving energy imparted to these resonant devices. This optical drive is sufficient to overcome the strong viscous damping present in these fluids, resulting in resonant motion that is detectable using interferometric techniques.

Beam-type resonators, both doubly and singly clamped, were fabricated with electron-beam (e-beam) lithography. These devices were made using FOX-16 as a negative e-beam resist, with a 100 keV exposure. The device substrate consisted of a 105-nm-thick stoichiometric silicon nitride layer, over an 800-nm-thick sacrificial oxide layer, on single-crystal silicon. After patterning, devices were etched in a CHF_3/O_2 plasma, released in buffered hydrofluoric acid, and then coated with a metal layer consisting of 5 nm Cr and 10−15 nm Au. The resulting devices ranged from 1 to 10 μm in length, 100 to 500 nm in width, and 120−125 nm in thickness. Figure 1 shows a scanning electron micrograph of a doubly clamped beam resonator with length 5 μm, width 150 nm, and thickness 125 nm. For resonance in liquid, chips are placed in a small fluid cell consisting of two pieces of plastic that press an O ring between a piece of cover glass and the device chip. Liquid is pipetted onto the chip within the O ring, the cover glass is then pressed onto the O ring, thereby sealing in the liquid, and the chip and glass are tightened together by the outer plastic pieces.

The optical drive and detection system used consists of an amplitude-modulated driving diode laser at 432 nm and a continuous wave detection laser at 633 nm. A spectrum

* Corresponding author. E-mail: hgc1@cornell.edu.
[†] Department of Physics and the Cornell Center for Materials Research.
[‡] School of Applied and Engineering Physics and the Cornell Center for Materials Research.

10.1021/nl061397t CCC: $33.50
Published on Web 08/18/2006

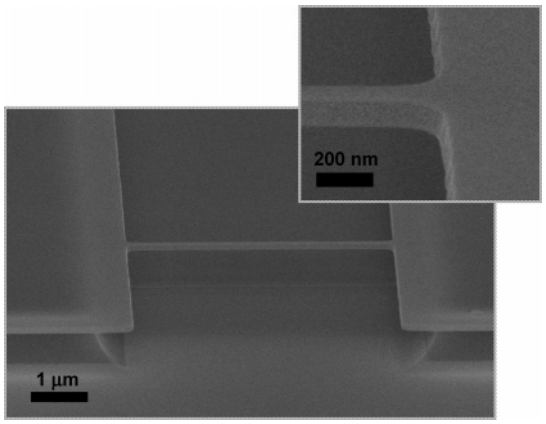

Figure 1. Scanning electron micrograph (SEM) image of a suspended metallized silicon nitride string. The string dimensions are 5 μm × 150 nm × 125 nm.

analyzer is used to sweep the amplitude modulation frequency (drive) of the blue laser, while monitoring the reflected red laser power detected by a photodiode. Modulating the amplitude of the driving laser at the appropriate frequency leads to resonant actuation of the device. This technique has been shown previously to work for single-material resonators made of either silicon or silicon nitride,[4] as a primarily thermal mechanism. This technique effectively drives our high-stress nitride devices in vacuum without a metal coating.[5] Bare nitride devices can be actuated in air with this technique, but with a thin metal coating the response is enhanced significantly. This enhancement is a combination of two effects. An increase in optical signal is observed for the more reflective metallized resonators. This is evident when signals from both metallized and nonmetallized beams are compared in vacuum, driven by piezo actuation at identical levels (piezo drive was found to ineffective for the nanoresonators studied in air and liquid environments, leading to large background levels that obscure resonance signals). In addition to this increase in signal, the optical drive mechanism is enhanced by the presence of the metal film. The metallized devices act as a bimorph material, with different thermal expansions for the silicon nitride and metal layers, leading to flexural displacement at the modulation frequency of the drive. Optical methods have been demonstrated previously for the effective drive and detection of nanomechanical resonators in air.[6] This particular use of amplitude-modulated laser drive with a bilayered beam has also been demonstrated for actuation of nanomechanical resonators in air.[7] We show that the effectiveness of this all-optical drive and detection technique resulting from the presence of a thin metal film not only enhances the signal in air but also makes it possible to actuate and detect nanomechanical resonators in liquids as well.

In Figure 2, we show the resonances of a pair of doubly clamped beams, in both air and liquid. These plots represent the amplitude of the AC component of the reflected detection laser over frequency ranges spanning the resonant frequencies of the beams. In Figure 2a is the resonance peak of a 2-μm-long, 165-nm-wide, and 125-nm-thick beam in air and water. In air, this device has a frequency of 145 MHz, with a quality

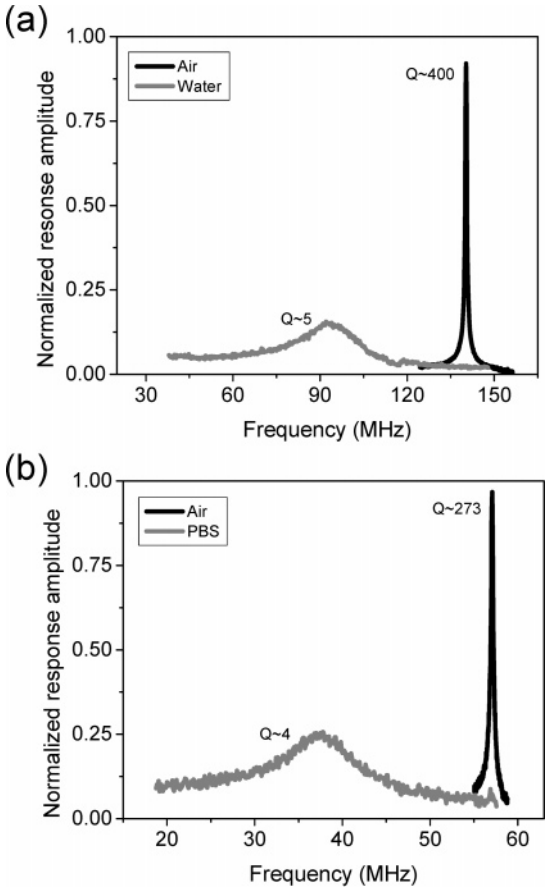

Figure 2. Normalized optical response of a pair of strings, representing the AC component of the reflected red detection laser power. The absolute, as well as relative, scales between peaks are arbitrary. A 2 μm × 165 nm × 125 nm string is shown in part a, with resonances in air (sharp peak, f = 145 MHz, Q = 400) and water (broad peak, f = 95 MHz, Q = 5). A 4 μm × 125 nm × 120 nm string is shown in part b, with resonances in air (sharp peak, f = 57 MHz, Q = 273) and phosphate-buffered saline (broad peak, f = 38 MHz, Q = 4).

factor (Q) of ~400. In water, the frequency is reduced to 95 MHz, with $Q \approx 5$. This reduction in Q is comparable to what has been observed with larger flexural resonators that have been operated in both air and liquid.[8,9] In Figure 2b is the resonance of a 4-μm-long, 125-nm-wide, and 120-nm-thick device in air and phosphate-buffered saline (PBS), with a frequency of 57 MHz in air and 38 MHz in buffer. The Q value for this device shrinks from 273 in air to 4 in buffer. This Q, and the demonstrated frequency shift from air to buffer, are comparable to what we see for the same device operated in water. This is a direct demonstration that devices of this scale can be operated in buffer solutions of relevance to biological molecules. Devices have also been resonated in isopropyl alcohol and acetone. Slightly higher Q values, up to 10, have been observed with resonance in acetone, which would be expected from the lower viscosity of acetone in comparison to water.

It has been observed that significant frequency shifts result from the operation of nanoscale resonators in liquids. It is interesting to consider the amount of added mass, in a simple model, to which these sorts of frequency shifts would

correspond. Consider the case of the 95 MHz resonator, whose response is displayed in Figure 2a. Assume for simplicity that the mass loading of the liquid does not alter the spring constant of the beam. Then we have the following relation between the initial frequency and mass (f, m), and final frequency and effective mass (f', m'):

$$\frac{f'}{f} = \sqrt{\frac{m}{m'}}$$

For this device, which has dimensions 2 μm × 165 nm × 125 nm, assuming a nitride density of 2700 kg/m^3 (which we have determined from frequency-length data for the silicon nitride used), we calculate a resonator mass of 1.1×10^{-16} kg. For the frequency−mass relationship given, a shift from 145 to 95 MHz would correspond to an added mass of 1.5×10^{-16} kg. Hence, a mass of fluid on the order of the mass of the resonator is entrained to the resonant motion. Consider fluid mass simply as a rectangular shell around the nitride beam, locked tightly to the motion of the resonator, with entrained fluid mass given by the simple geometric equation

$$m' - m = \{(w + 2\Delta x)(t + 2\Delta x) - wt\} \times l \times \rho_{\text{liquid}} = \{2(w + t)\Delta x + 4\Delta x^2\} \times l \times \rho_{\text{liquid}}$$

in terms of width w, thickness t, length l, and liquid penetration depth Δx from the resonator surface. For the 95 MHz resonator, given an added liquid mass of 1.5×10^{-16} kg, solving this equation yields $\Delta x \approx 82$ nm. From basic considerations of an incompressible viscous fluid,[10] we would expect that a device resonating in liquid should have a viscous penetration depth into the surrounding medium given by the equation

$$\delta = \sqrt{\frac{2\upsilon}{\omega}}$$

where υ is the kinematic viscosity of the surrounding medium (defined as the ratio of dynamic viscosity, η to density, ρ) and ω is angular frequency. For a resonance at 95 MHz in water ($\upsilon \approx 1 \times 10^{-6}$ m^2/s at room temperature), $\delta \approx 58$ nm, comparable to the 82 nm result from the simple consideration given above. Thus, the resonator plus entrained fluid comprises an "effective resonator" whose dimensions are only slightly larger (on the order of 100 nm) than the dimensions of the nanobeam itself. It should be noted that we do not differentiate between a "natural" resonant frequency, and a "damped" resonant frequency for our devices. As Q approaches order unity, this becomes an important distinction to make. But even for $Q \approx 3$, these two frequencies differ by less than 3%, and hence do not significantly change our correlations of frequency shift to mass loading.

In the bottom panel of Figure 3, we show data for frequency as a function of inverse length for two sets of doubly clamped beam resonators, with average widths of 175 nm (±25 nm) and lengths from 2 to 6 μm, as well as identical length beams with 500 nm (±25 nm) widths. These resonators are made from a silicon nitride material with very high tensile stress, ~1200 MPa, so the frequencies are expected to be proportional to inverse length. Operation of high-tensile-stress nitride devices in vacuum has been discussed elsewhere.[5] Without a metal layer, these devices demonstrate quality factors as high as 200 000 in vacuum for resonator lengths of 60 μm, at room temperature. In vacuum, a 20 nm metal layer reduces Q significantly. In gaseous environments, where viscous damping is the dominant loss mechanism, no difference in quality factor between metallized and nonmetallized devices is evident. It is clear in Figure 3 that there is a systematic frequency shift when beams operated in air and water are compared for devices of all lengths (and hence frequencies) considered. The linear dependence on inverse length holds fairly well in both air and water. The ratio of frequency in liquid to frequency in air, f'/f, is also shown to be essentially constant for the lengths of resonator considered, and for a given width, as shown in the top panel of Figure 3. This ratio, however, depends on beam width at all frequencies considered and is inconsistent with the simple picture of mass loading we have described in which there is only a viscously coupled mass that gives rise to the frequency shift. If this were the case, then we would expect that

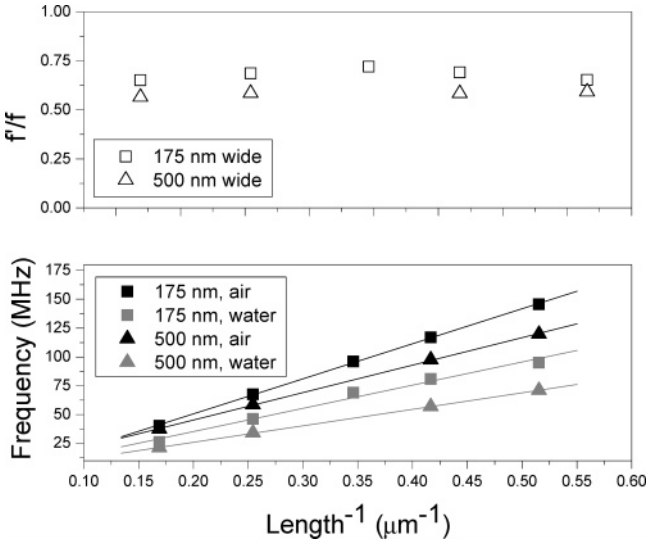

Figure 3. A plot of frequency vs inverse length for strings of widths 175 (±25) nm and 500 (±25) nm is shown in the bottom panel, for operation in both air and water. The ratio of frequency in water (f') to frequency in air (f) is shown in the top panel for these two sets of strings.

$$\frac{f'}{f} = \sqrt{\frac{m}{m'}} = \sqrt{\frac{m_{\text{beam}}}{m_{\text{beam}} + m_{\text{viscous}}}}$$

where m_{viscous} is interpreted as the mass of the fluid shell viscously "locked" to the beam, penetrating a distance, $\delta \equiv$ viscous penetration depth, into the fluid. The beam mass m is linear in width, whereas the viscous mass, in the geometric model described, would be a sum of three terms, one of which is linear in width, with the other terms independent

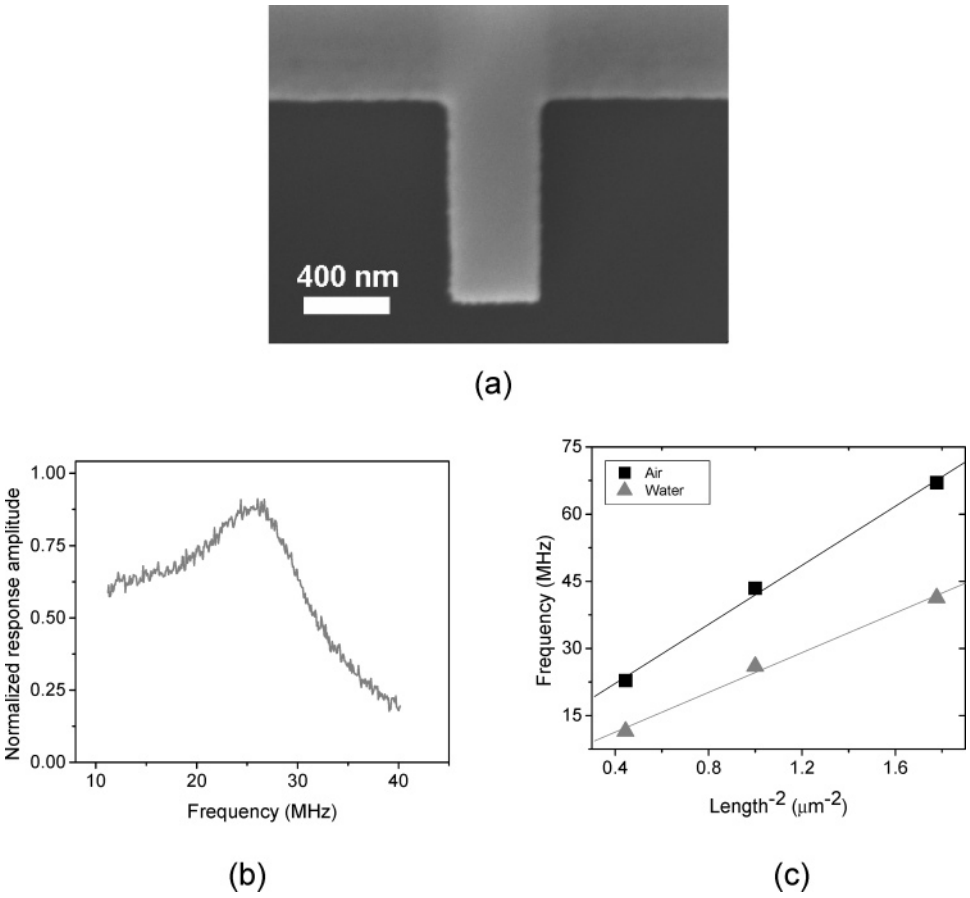

Figure 4. An optical response curve for a 1 μm × 450 nm × 125 nm cantilever is shown in part b, with an SEM of a similar device shown in part a. A plot of frequency vs the square of inverse length is shown in part c for cantilevers of length 1.5 μm, 1 μm, and 750 nm, and width 450 nm.

of width. Therefore f'/f should increase for increasing beam width within this simple viscous model. From the upper panel of Figure 3, however, it is clear that this is not the case, and in fact the wider beams are observed to have smaller values of f'/f. In reality, this observed frequency shift is not only a result of viscous effects. There is an inertial term that must also be considered, which is related to the volume of fluid the resonator must displace during its motion.[11] This term is manifested as an extra mass term, yielding

$$\frac{f'}{f} = \sqrt{\frac{m_{\text{beam}}}{m_{\text{beam}} + m_{\text{viscous}} + m_{\text{inertial}}}}$$

The precise form of both the viscous and inertial terms would depend on the cross-sectional geometry of the resonator being considered, as well as additional factors including surface roughness and surface hydrophobicity, which might alter the boundary conditions relevant to the system.[12] Such a careful analysis would yield important information for precisely understanding the performance of liquid-compatible sensors built from these resonators

Singly clamped beams of the same nanoscale dimensions have also been studied, with quality factors and frequency shifts comparable to those observed for the doubly clamped beams. A response peak for a 450-nm-wide, 1-μm-long, and 125-nm-thick cantilever beam is shown in Figure 4b, with an SEM of a beam of this size in Figure 4a. Frequency is plotted against length for cantilevers with lengths of 750 nm, 1 μm, and 1.5 μm in Figure 4c, showing the expected proportionality of frequency to the *square* of inverse length.

Nanoscale resonators that can be driven and detected with all optical techniques in gas and liquid have potential utility in a number of applications. Resonators of such small masses that can be operated in air with quality factors of several hundred could be quite useful for chemical sensing in ambient environments, making costly vacuum packaging unecessary. Although the quality factors of these devices operated in liquid are small (on the order of 5), they might also be useful for the sensing of biological molecules in liquid. Consider once again the 95 MHz resonator already presented. This device, including entrained liquid, has a mass of 2.6×10^{-16} kg. The resonant frequencies of several of our resonators of this size and frequency operated in water have observed stabilities of better than 1 MHz for tens of minutes, without considering temperature fluctuations that limit the frequency stability of these high-stress devices. Shown in Figure 5 is a series of resonant peaks for a 300-nm-wide string, with $Q \approx 4$, resonating at ~57 MHz in water. Representative peaks are shown for 0, 4, 7, and 10 min (the amplitudes have been scaled to make the peaks clearly distinguishable). Frequency was measured at 8 points

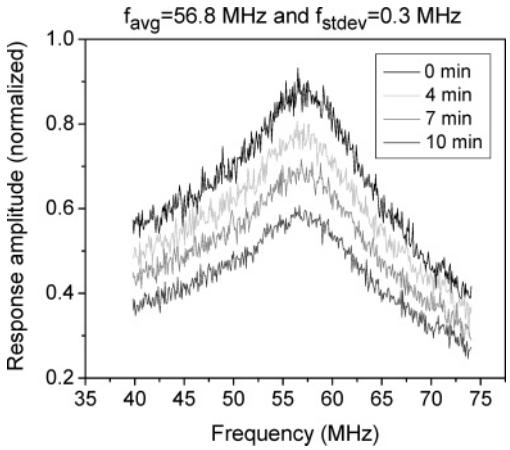

Figure 5. Overlay of four different response peaks for a 300-nm-wide, 57 MHz doubly clamped beam resonator with $Q \approx 4$. Peaks shown represent resonance at $t = 0$, 4, 7, and 10 min. The average frequency over this time period (eight frequency measurements taken in total, each from a Lorentzian fit to an average of ten 0.5 s sweeps over the frequency range shown) was 56.8 MHz, and the standard deviation was 0.3 MHz.

in time spread out during this 10 min period, by fitting a Lorentzian to the peak and extracting the center frequency. Each peak represents an average of 10 sweeps of the spectrum analyzer over the range shown in Figure 5, with each sweep taking 0.5 s. The average frequency obtained over this 10 min period was 56.8 MHz, with a standard deviation of 0.3 MHz. Hence, a 1 MHz shift represents 3 times the standard deviation in the average frequency for this device over a 10 min period. A frequency resolution of this magnitude for our highest frequency resonator is equivalent to an added mass of $\sim 10^{-18}$ kg, or 1 femtogram (fg), corresponding to the mass of a single medium-sized virus, and is comparable to the state of the art in terms of absolute minimum measurable mass as performed with flexural beam-type resonators operated in air,[13,14] as well as electrical nanowire detection in liquid.[15] Detection in liquid could allow for real-time measurement of individual binding events and perhaps even direct measurement of nonequilibrium binding information that might not be accessible using other techniques. Operation in biocompatible liquids could also preserve the full biological form and function of the molecules being detected, avoiding potentially harmful drying out of these molecules.

Because of the small size of the nanobeam resonators, thousands of devices can readily be placed within the on-chip real-estate typically occupied by a single quartz crystal microbalance (QCM), which is on the order of millimeters on a side, and is the typical tool of choice for sensitive mass detection in gas and liquid environments. Hence, arrays of nanobeam resonators could be used to produce enhanced surface sensitivity or mass sensitivity per unit area by creating a large number of mass-sensitive resonator pixels.

Optical drive and detection for mechanical resonators is attractive for operation in liquid for a number of reasons. This noninvasive technique avoids any possible complications that could arise from operating electrical elements in conducting liquid environments, where electrical shorting, and even electrochemical reactions could occur, complicating interfacing to these devices. Our demonsration of an all-optical actuation and detection system for nanomechanical resonators in liquid might also prove technologically useful for AFM imaging. We found piezo actuation to be an ineffective drive technique for the operation of our nanoscale resonators in air and liquid, with background levels associated with high piezo drive level obscuring the small resonant signals from our devices. Laser drive, which has been shown here to be effective in liquid for both doubly clamped beams and cantilevers, might similarly be more effective than piezo drive for the actuation of traditional AFM cantilevers in liquid, as well as cantilevers of shrinking dimensions.

In all of the applications discussed, quality factors higher than those demonstrated in this letter would be useful. We propose that a nonlinear feedback technique could be used to increase the quality factors of these nanoresonators by 1 or 2 orders of magnitude, yielding higher force sensitivities when combined with improved thermal stabilization of resonant frequency. This technique has been used to enhance the quality factors of cantilever resonators used for atomic force microscopy,[2] and effective quality factors exceeding 1000 in air for nanomechanical resonators have been obtained using a parametric amplification technique.[6]

In conclusion, we have demonstrated that an all-optical drive and detection system can be used for the operation of flexural nanomechanical resonators in air, as well as viscous fluids including alcohol, water, and buffer. Bilayered nanobeams of Au/Cr on silicon nitride have been driven into resonance by modulating the amplitude of a focused blue laser at the appropriate frequency, leading to differential expansion of the device materials and a harmonic flexural displacement at the drive modulation frequency. An interferomentric technique using a red laser was then used to detect the motion of beams with cross sections on the scale of 100 nm, at radio frequencies. Quality factors in air as high as 400 at 145 MHz, and in liquid from 3 to 10 with frequencies from 20 to 100 MHz, have been demonstrated. It has been shown that the mass of the fluid entrained to the motion of these devices is on the scale of the device mass itself, with a single resonant device having the potential to detect a single femtogram mass in real time. The potential for increasing the force sensitivity of these devices by increasing effective quality factors with nonlinear drive techniques, as well as creating arrays of many such mass-sensitive pixels to increase mass sensitivity per unit area, has been discussed. These devices, and the all-optical drive and detection system used, greatly extend the viscosity range over which such sensitive resonant devices can be operated, potentially providing insight into the physics of the interaction of such small mechanical devices with their environments.

Acknowledgment. The e-beam lithography was performed and the thin films were deposited and characterized at the Cornell Nano-Scale Science & Technology Facility. Research was supported by the CCMR under NSF Grant DMR 0520404.

References

(1) Ilic, B.; Craighead, H. G.; Krylov, S.; Senaratne, W.; Ober, C.; Neuzil, P. *J. Appl. Phys.* **2004**, *95*, 3694.
(2) Tamayo, J.; Humphris, A. D. L.; Owen, R. J.; Miles, M. J. *Biophys. J.* **2001**, *81*, 526−537.
(3) Xu, Y.; Lin, J. T.; Alphenaar, B. W.; Keynton, R. S. *Appl. Phys. Lett.* **2006**, *88*, 143513-1−3.
(4) Ilic, B.; Krylov, S.; Aubin, K.; Reichenbach, R.; Craighead, H. G. *Appl. Phys. Lett.* **2005**, *86*, 193114-1−3.
(5) Verbridge, S. S.; Parpia, J. M.; Reichenbach, R. B.; Bellan, L. M.; Craighead, H. G. *J. Appl. Phys.* **2006**, *99*, 124304.
(6) Sekaric, L.; Zalalutdinov, M.; Bhiladvala, R. B.; Zehnder, A. T.; Parpia, J. M.; Craighead, H. G. *Appl. Phys. Lett.* **2002**, *81*, 2641−2643.
(7) Sampathkumar, A.; Murray, T. W.; Ekinci, K. L. *Appl. Phys. Lett.* **2006**, *88*, 223104-1−3.
(8) Vignola, J. F.; Judge, J. A.; Jarzynski, J.; Zalalutdinov, M.; Houston, B. H.; Baldwin, J. W. *Appl. Phys. Lett*. **2006**, *88*, 041921-1−3.
(9) Yum, K.; Wang, Z.; Suryavanshi, A. P.; Yu, M. F. *J. Appl. Phys.* **2004**, *96*, 3933−3938.
(10) Landau, L. D.; Lifshitz, E. M. *Fluid Mechanics*; Butterworth-Heinemann: 2003; p 83−88.
(11) Guenault, A. M.; Keith, V.; Kennedy, C. J.; Pickett, G. R. *Phys. Rev. Lett.* **1983**, *50*, 522−525.
(12) Bowley, R. M.; Owers-Bradley, J. R. *J. Low Temp. Phys.* **2004**, *136*, 15−38.
(13) Gupta, A.; Akin, D.; Bashir, R. *Appl. Phys. Lett.* **2004**, *84*, 1976−1978.
(14) Lavrik, N. V.; Datskos, P. G. *Appl. Phys. Lett.* **2003**, *82*, 2697−2699.
(15) Patolsky, F.; Zheng, G.; Hayden, O.; Lakadamyali, M.; Zhuang, X. *Proc. Natl. Acad. Sci.* **2004**, *101*, 14017−14022.

NL061397T